Supporting Information for

Evaluation of reanalysis soil moisture products using Cosmic Ray Neutron Sensor observations across the globe

Yanchen Zheng[1,2], Gemma Coxon[1], Ross Woods[2], Daniel Power[2], Miguel Angel Rico-Ramirez[2], David McJannet[3], Rafael Rosolem[2,4], Jianzhu Li[5] and Ping Feng[5]

[1]School of Geographical Sciences, University of Bristol, Bristol, UK.

[2]Department of Civil Engineering, University of Bristol, Bristol, UK.

[3]CSIRO Environment, EcoSciences Precinct, Dutton Park, Queensland, Australia.

[4]Cabot Institute for the Environment, University of Bristol, Bristol, UK.

[5]State Key Laboratory of Hydraulic Engineering Simulation and Safety, Tianjin University, Tianjin, China.

Corresponding to: Yanchen Zheng (yanchen.zheng@bristol.ac.uk)

Contents of this file

Introduction

The supporting Information provides additional information and analysis that are not directly related to the main conclusions.

Text S1. The timeseries comparison for 4 same UK sites from COSMOS-UK and COSMOS-Europe

There are 4 same sites, namely EUSTN, FINCH, LULLN and GLENS, from COSMOS-UK and COSMOS-Europe networks. COSMOS-UK datasets provide both hourly and daily soil moisture data (Evans et al. 2016, Cooper et al. 2021), whereas COSMOS-EU datasets provide the hourly data (Bogena et al. 2022). We first compare timeseries data from two CRNS networks at hourly scale, and then we also aggregate the hourly COSMOS-Europe data to daily scale for the comparison with COSMOS-UK daily data. Figure S1 and Figure S2 display the soil moisture timeseries for these 4 UK sites from two CRNS networks at hourly and daily scale.

In general, the differences of the soil moisture data from two datasets at hourly scale are larger than that of at daily scale. The differences of one site in Scotland named GLENS is large. The hourly data from COSMOS-UK for this site have large variability than that of COSMOS-Europe. Statistical metrics, i.e., bias and Pearson correlation coefficient (R), are adopted to quantify the differences between two networks. The results shows that the bias is smallest for site FINCH at both hourly and daily scale, while the temporal correlation have best performance at site EUSTN. Yet, for site GLENS, the worse performance is notable in terms of bias and R values. The temporal correlation between COSMOS-UK and COSMOS-Europe is less than 0.5 at hourly scale. This deviation highlights the importance of processing harmonized CRNS datasets for the evaluation.

Table S1. Statistical metric values for 4 UK sites

Scale	Sites	Bias	R
Hourly	EUSTN	-0.01	0.956
	FINCH	0.01	0.880
	LULLN	0.03	0.856
	GLENS	0.06	0.447
Daily	EUSTN	-0.01	0.999
	FINCH	0.00	0.996
	LULLN	0.03	0.985
	GLENS	0.03	0.820

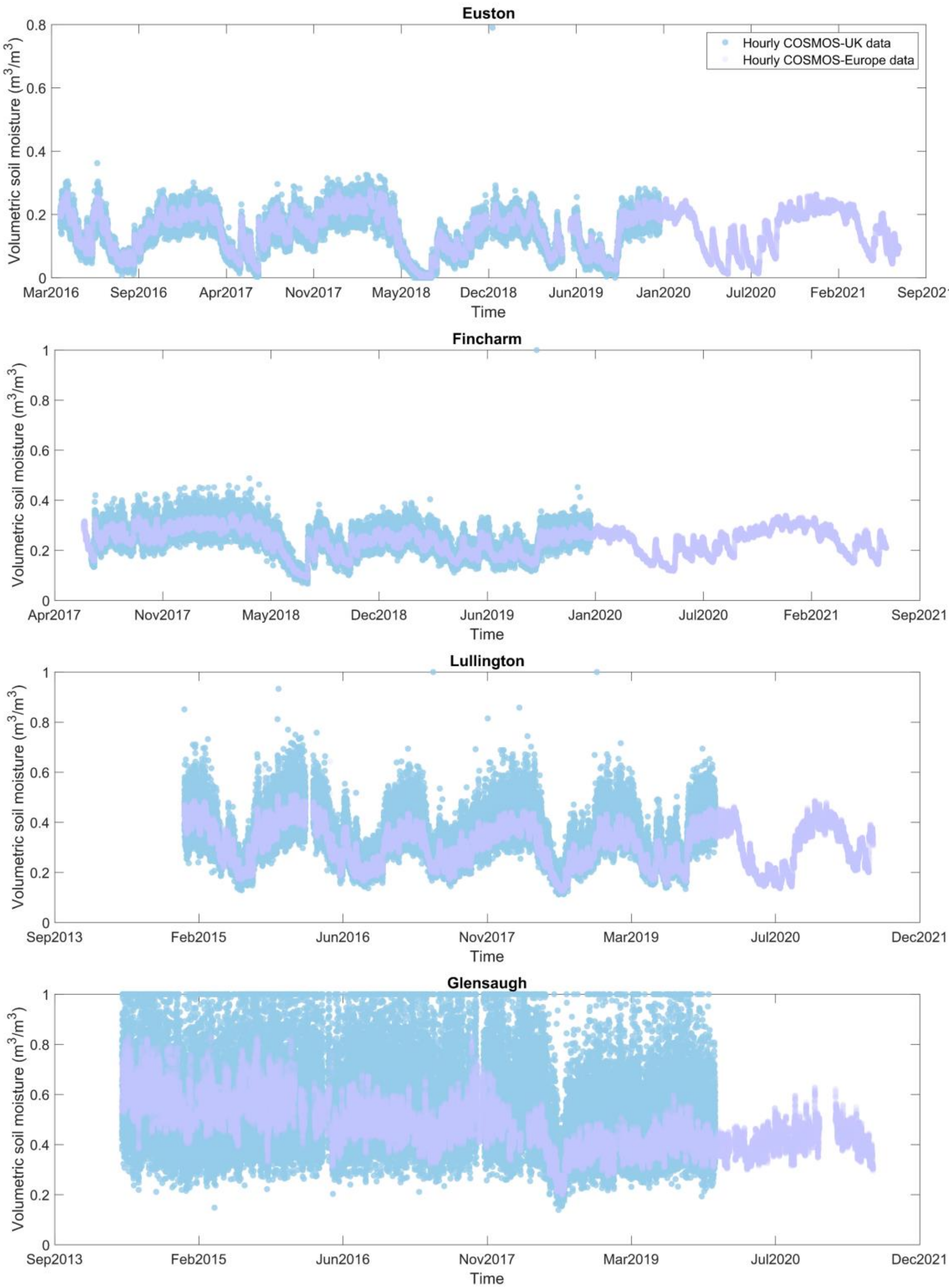

Figure S1. Soil moisture timeseries comparison for 4 same UK sites from COSMOS-UK and COSMOS-Europe networks at hourly scale

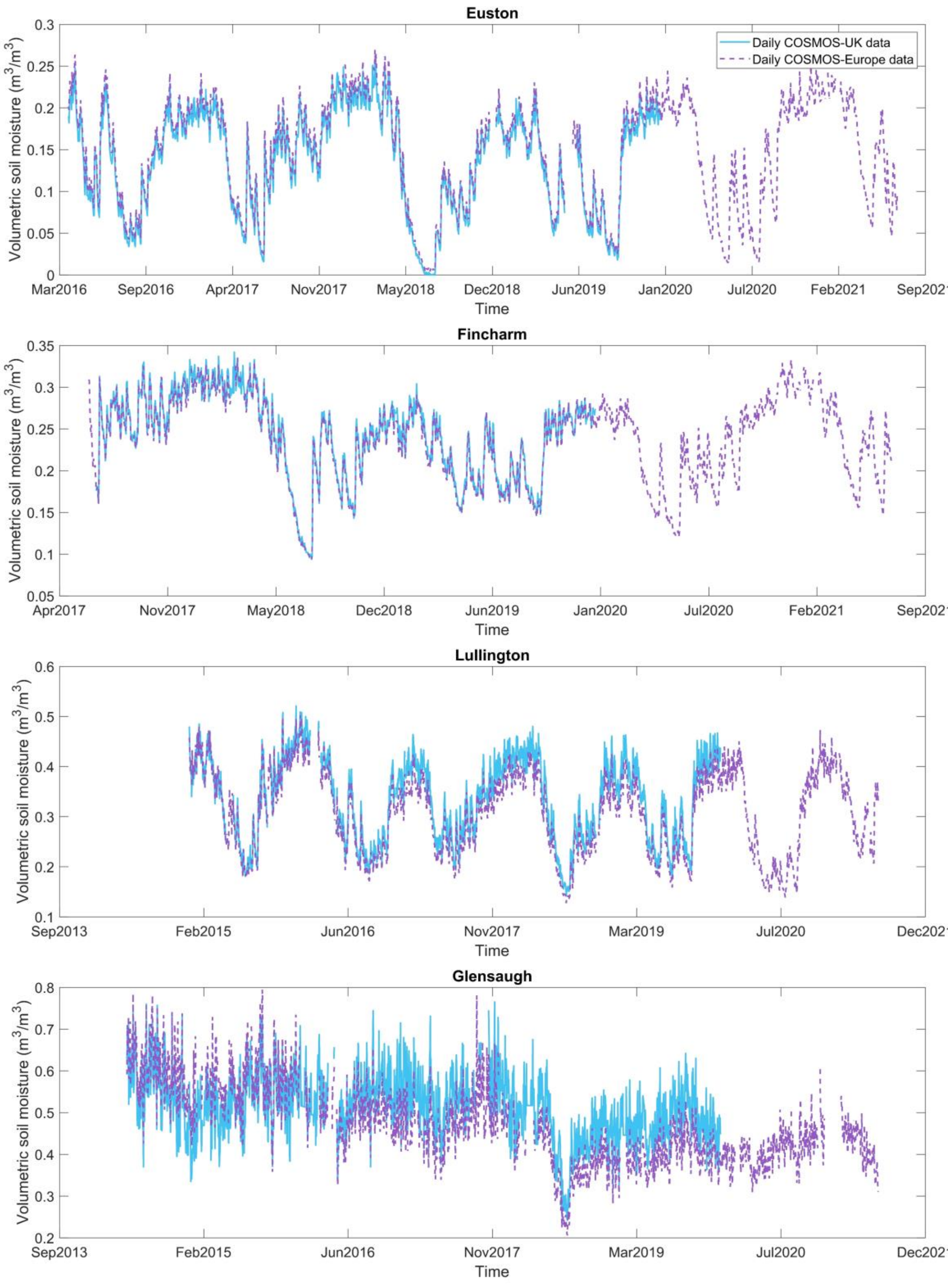

Figure S2. Soil moisture timeseries comparison for 4 same UK sites from COSMOS-UK and COSMOS-Europe networks at daily scale

Text S2. Reprocessing COSMOS USA and CosmOz data using crspy

The COSMOS (USA) and CosmOz (Australia) networks have more clear deviations in how they process CRNS data, when compared to COSMOS-UK and COSMOS-EUROPE. To account for this raw CRNS data was collected from the respective networks and reprocessed through crspy (Power et al. 2021) to ensure the soil moisture values came from a comparable methodology. This is indeed possible as both networks maintain and provide raw CRNS data that can be reprocessed if required.

In the case of COSMOS (USA) the network was initially set up without external sensors for temperature and relative humidity. Since the network was established an understanding of the influence atmospheric water vapour has on the neutron counting rate has led to methods to account for this (Rosolem et al. 2013, Köhli et al. 2021). The current standard is to use the Rosolem et al. (2013) method, which requires a method to give an estimate/reading of absolute humidity. As most USA sites do not have external temperature and relative humidity sensors to do this, crspy contains a method to use ERA5-Land data (specifically using temperature_2m and dewpoint_temperature_2m values) to derive absolute humidity estimates. Although ideally in-situ data would lead to more accurate corrections to the neutron signal, it has been shown that using ERA5-Land data is clearly preferable to not correcting for atmospheric water vapour at all (Power et al. 2021). In addition, the development of crspy is motivated by multi-site processing covering the globe, hence the choice of a common global product rather than relying on the availability or not of local/national meteorological monitoring stations.

The CosmOz network was initially set up in the same way as the COSMOS-USA network, without external temperature and relative humidity sensors. In 2016 the original sites had these sensors installed and sites that have been installed since 2016 have in-situ sensors available to correct for atmospheric water vapour. As we were missing sensor data prior to 2016, the decision was made to follow the methodology taken with the COSMOS-USA sites, and all the CosmOz sites were processed using ERA5-Land data to account for atmospheric humidity. Additionally, the CosmOz network uses a different method to account for high energy incoming neutrons (Hawdon et al. 2014). Instead of using the Jungfraujoch station as a reference, with a correction to account for differences in cut-off rigidity between the reference site and the CRNS site, the CosmOz network selects a neutron monitoring site with a similar cut-off rigidity to the CRNS site being corrected. There are arguments about which method is optimal and this requires further research. For the purposes of this study, and to ensure a harmonized processing method, the CosmOz data was reprocessed through crspy with the incoming neutron intensity correction set to match the methods from COSMOS-UK and COSMOS-Europe.

Text S3. Detailed descriptions of 7 reanalysis soil moisture products

S3.1 ERA5-Land

ERA5-Land is an enhanced global dataset for the land component of the fifth generation of European Reanalysis (ERA5) developed by the European Centre for Medium-Range Weather Forecasts (ECMWF). ERA5-Land data is produced through global high-resolution numerical integrations of the ECMWF land surface model driven by the downscale meteorological forcing from the ERA5 climate reanalysis. With enhanced description of the hydrological cycle, especially the soil moisture and lake description, ERA5-Land exhibited better agreement of river discharge estimations compared to available observations (Muñoz-Sabater et al. 2021). The main advantage of ERA5-Land compared to its predecessors (i.e., ERA5 and ERA-Interim dataset) is the finer horizontal resolution. ERA5-Land dataset provides hourly data at a spatial resolution of 0.1° (~9km) on global land surface for more than 70 years, which makes this product widely used (Xu et al. 2022). ERA5-Land data is accessible at https://www.ecmwf.int/en/era5-land.

S3.2 CFSv2

CFSv2 is the second version of the National Centers for Environmental Prediction (NCEP) Climate Forecast System (CFS). CFS is a fully coupled model simulating the interaction between the Earth's atmosphere, oceans, land and sea ice (Saha et al. 2010), which provides reanalysis data spanning from 1979 to 2010. CFSv2 was upgraded and made operational at NCEP in March 2011. Substantial upgrades to nearly all aspects of the data assimilation and forecast model components of the system have been made (Saha et al. 2014), with results showing that CFSv2 achieved significant improvement against CFSv1 and better potential in forecasting precipitation, soil moisture values (Yuan et al. 2011, Yuan et al. 2013, Saha et al. 2014). CFSv2 data can be downloaded from https://rda.ucar.edu/datasets/ds094.1/.

S3.3 MERRA-2

MERRA-2 (GMAO 2015) is the latest version of the global atmospheric reanalysis dataset released by NASA Global Modeling and Assimilation Office (GMAO) using the Goddard Earth Observing System Model (GEOS),. Numerous improvements have been made in the assimilation system for producing the MERRA-2 dataset, including the assimilation of modern hyperspectral radiance and microwave observations (Gelaro et al. 2017, Reichle et al. 2017). MERRA-2 is the first global reanalysis to assimilate aerosol measurements as well as their interaction with other physical process. More details about MERRA-2 can be found from https://gmao.gsfc.nasa.gov/reanalysis/MERRA-2/.

S3.4 JRA-55

The Japanese 55-year Reanalysis (JRA55) project is launched by the Japan Meteorological Agency in 2010, which is a successor of the Japanese 25-year Reanalysis (JRA25). JRA55 is the first reanalysis product to adopt a four-dimensional variational (4D-Var) analysis as its data assimilation scheme (Kobayashi et al. 2015). Additionally, model spatial resolution, newly available observational data sources and new radiation scheme have been applied in JRA55 to address several deficiencies in JRA25, and to provide a high-quality comprehensive atmospheric dataset from 1958. The mass concentration of condensed water in the soil (kg/m^3) are available in JRA55, which can be divided by the density of water to acquire the volumetric soil water data. The thickness of each soil layer in JRA55 data varies with the vegetation and land covers type. JRA55 data is given at https://rda.ucar.edu.

S3.5 GLDAS-Noah

The Global Land Data Assimilation System Version 2 (GLDAS2) is developed by a joint contribution of NASA's Goddard Space Flight Center and NOAA's National Centers for Environmental Prediction (NCEP). GLDAS-Noah v2.1 is driven with a combination of model and observation data. The forcing data include Global Precipitation Climatology Project (GPCP) version 1.3 dataset with 3-4 month latency. GLDAS-Noah v2.1 has been frequently used as a reference dataset for merging or evaluating satellite soil moisture products (Liu et al. 2011, Kim et al. 2018, Gruber et al. 2020). GLDAS-Noah v2.1 data is available from https://disc.gsfc.nasa.gov/.

S3.6 CRA40

CRA40 is the first-generation global reanalysis product produced by the China Meteorological Administration (CMA). The CRA40 project was launched in 2014 and released data recently (Liu et al. 2017). The CRA40 employs the 3D-Var data assimilation system from GFS/GSI (Global Forecast System/Gridpoint Statistical Interpolation) of NCEP. Multiple source data from conventional observations and satellite products, especially more observations from China and other East Asia regions, have been assimilated into CRA40 reanalysis product (Yu et al. 2021, Zhao et al. 2021). CRA40 can be obtained from http://data.cma.cn/.

S3.7 GLEAM

The Global Land Evaporation Amsterdam Model (GLEAM) estimates the terrestrial evaporation as well as surface and root-zone soil moisture based on satellite forcing data (Miralles et al. 2011, Martens et al. 2017). In particular, the GLEAM v3.5a dataset is based on reanalysis radiation and air temperature, satellite-based vegetation optical depth and a multi-source precipitation product. The GLEAM v3.5a provides daily gridded surface (0-10cm) and root-zone soil moisture data, which is available at https://www.gleam.eu/. The soil layer depth of root-zone varies depending on different land cover types.

Text S4. List of 135 CRNS sites used in this study

General information, including geographic locations, elevation, land cover type and start date, of 135 CRNS sites selected in this study is summarized in Table S2. The detailed data for each site including climate, soil properties and slope is provided in the 'CRNSsiteData.xlsx' of the supplementary files.

Text S5. Comparison results of three vertical scale mismatch processing methods

Three different methods are tested to solve the vertical mismatch between CRNS measurements and reanalysis products. The details of these three methods are listed as follows:

a) V1: Only select the soil moisture data of the layer where D86 (see definition from (Köhli et al. 2015)) is located;

b) V2: Equally average of all the soil layers up to D86;

c) V3: Assign weights to all the soil layers up to D86.

The formula for calculating the vertical weights in V3 method can be found in section 3.1.3 of the main paper.

In general, the calculated soil moisture data for almost all sites by using V2 and V3 are highly similar to each other. Taking one UK site, i.e., EUSTN, as an example, Figure S3a compares the soil moisture timeseries data for three vertical processing methods from ERA5-Land and CRNS observations. The table (Figure S3b) shows the performance quantified by R and RMSE values. It is clear that soil moisture timeseries processed by V1 exhibit worse performance on both statistical metrics. The extracted reanalysis soil moisture series by using V2 and V3 present better temporal dynamic than that of V1, especially in the dry condition.

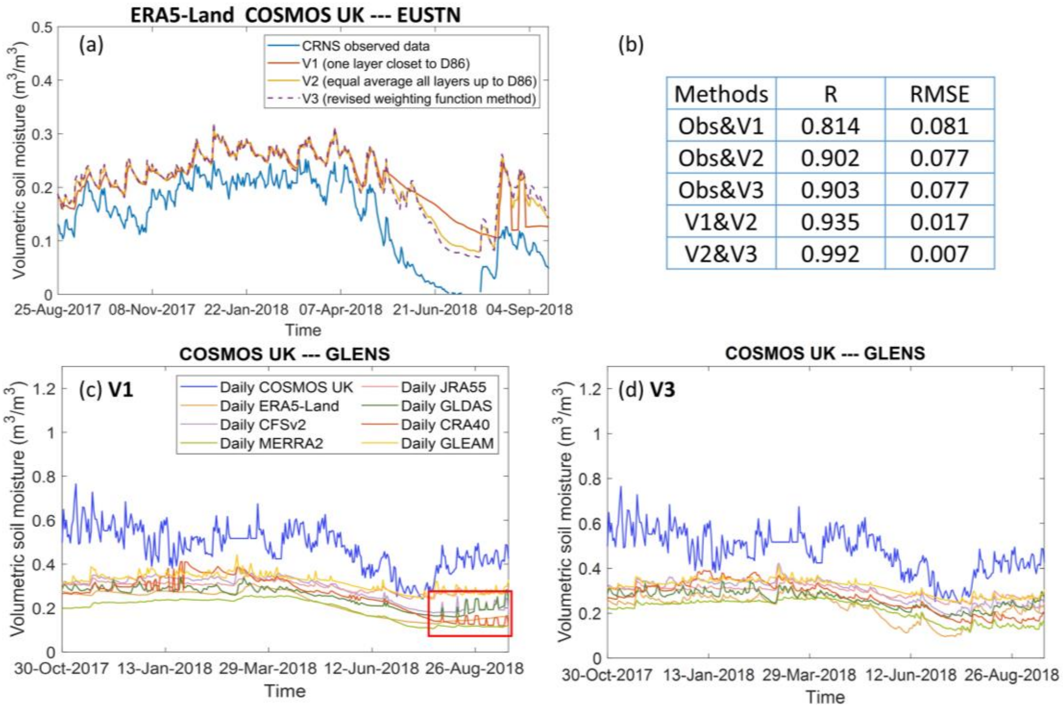

Methods	R	RMSE
Obs&V1	0.814	0.081
Obs&V2	0.902	0.077
Obs&V3	0.903	0.077
V1&V2	0.935	0.017
V2&V3	0.992	0.007

Figure S3. Comparison results for three different vertical processing methods.

Figure 3c, d display the processed soil moisture daily timeseries from all reanalysis products and CRNS measurements at GLENS UK site under V1 and V3 method, respectively. As for V1 method, since the selection of soil layers varies with the D86 at each time step, the abrupt change in selecting different soil layers leads to several spikes in soil moisture timeseries data. In contrast, the soil moisture timeseries from V3 method exhibit natural variations against CRNS measurements.

Text S6. Performance of reanalysis products summarized in boxplots for 6 statistical metrics

Performance of the 7 SM reanalysis products in terms of 6 statistical metrics for 4 different regions are summarized in boxplots (Figure S4 and Figure S5). The recommended top two products are showed in green colour, while the red boxes represent the products with the worst performance. The rest of the products are displayed in yellow colour. Overall, the performance of reanalysis products varies across different regions.

Figure S4. Performance of the 7 SM reanalysis products in terms of *R*, *Rsea* and *Rano* statistical metrics for 4 regions.

Figure S5. Performance of the 7 SM reanalysis products in terms of *MSE*, *ubRMSE* and *Bias* statistical metrics for 4 regions.

Text S7. Average Brunke ranking scores for 7 reanalysis SM products

The derived statistic metric for each site across different products are provided in 'StatisticMetric.xlsx' of the supplementary files. Table S3 presents the average Brunke ranking scores for 7 reanalysis SM products under various regions, climate, land cover and topographic slope conditions. Details of how to calculate the average Brunke ranking scores are presented in section 3.3 of the main paper.

Table S3. Average Brunke ranking scores for 7 reanalysis SM products.

Class	Type	ERA5-Land	CFSvs2	MERRA2	JRA55	GLDAS-Noah	CRA40	GLEAM
Region	UK (45 sites)	3.57	**2.99**	4.36	4.35s	4.62	3.79	**3.49**
	EU (41 sites)	**2.64**	3.64	4.87	4.15	4.29	4.00	3.89
	USA (38 sites)	3.71	4.73	4.03	4.46	4.34	**3.11**	**3.47**
	AUS (11 sites)	5.15	**3.00**	3.64	4.61	4.11	3.53	**3.29**
Climate	Humid (53 sites)	**2.93**	**3.34**	4.65	3.96	4.51	4.19	3.72
	Balanced (42 sites)	3.70	**3.48**	4.56	4.43	4.32	3.56	3.62
	Arid (40 sites)	3.91	4.44	3.78	4.73	4.33	**2.99**	**3.38**
Land cover	Forest (33 sites)	3.58	4.21	4.24	4.20	4.30	**3.12**	3.81
	Cropland (41 sites)	**3.29**	3.68	4.68	4.12	4.35	3.91	3.57
	Shrubland (20 sites)	3.83	4.06	3.89	4.63	4.65	**3.30**	**2.97**
	Grassland (41 sites)	**3.36**	**3.14**	4.37	4.55	4.41	3.90	3.72
Slope	Steep (55 sites)	**3.49**	3.64	4.29	4.31	4.42	**3.49**	3.68
	Flat (80 sites)	**3.44**	3.74	4.41	4.37	4.39	3.72	3.52

Note: The bold numbers in green represent the relatively good performance with the Brunke ranking scores <3.5 (**recommended**), numbers with light green shading denote its Brunke ranking scores within 3 (**highly recommended**). The numbers in red with underline indicate the worst performance across all reanalysis products (not recommended).

Text S8. Spatial map of average statistical metrics performance of all 7 products

Figure S6 and S7 provide the spatial map of average all 7 products performance in terms of *Rsea*, *Rano* and *MSE*, *ubRMSE*, respectively. The spatial distribution of *Rsea* is similar with that of *R*. The performance of *Rano* is generally worse than the correlation of original and seasonal SM time series. No clear spatial pattern is observed in the USA and Australia in terms of *MSE* and *ubRMSE*, while several sites with high *MSE* and *ubRMSE* values are notable in the UK.

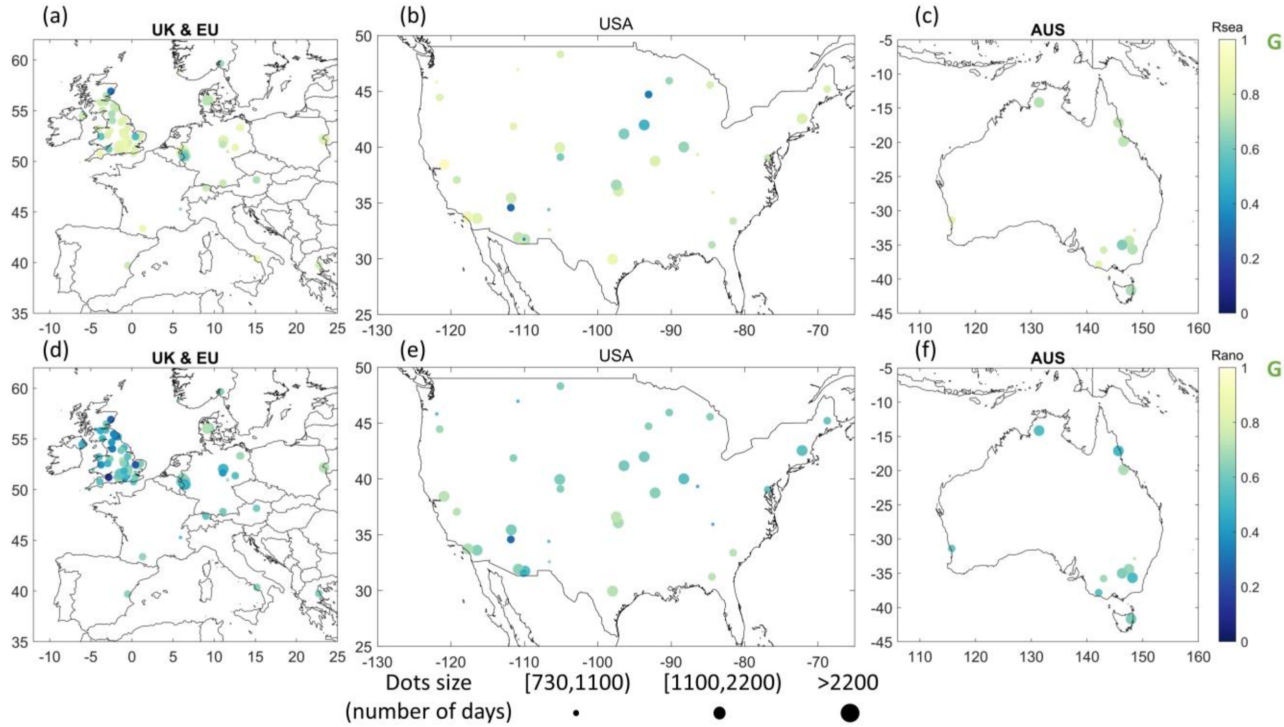

Figure S6. Spatial distribution of average statistical metrics *Rsea* and *Rano* performance of all 7 products. The green letter G denotes the statistical metric values with good performance.

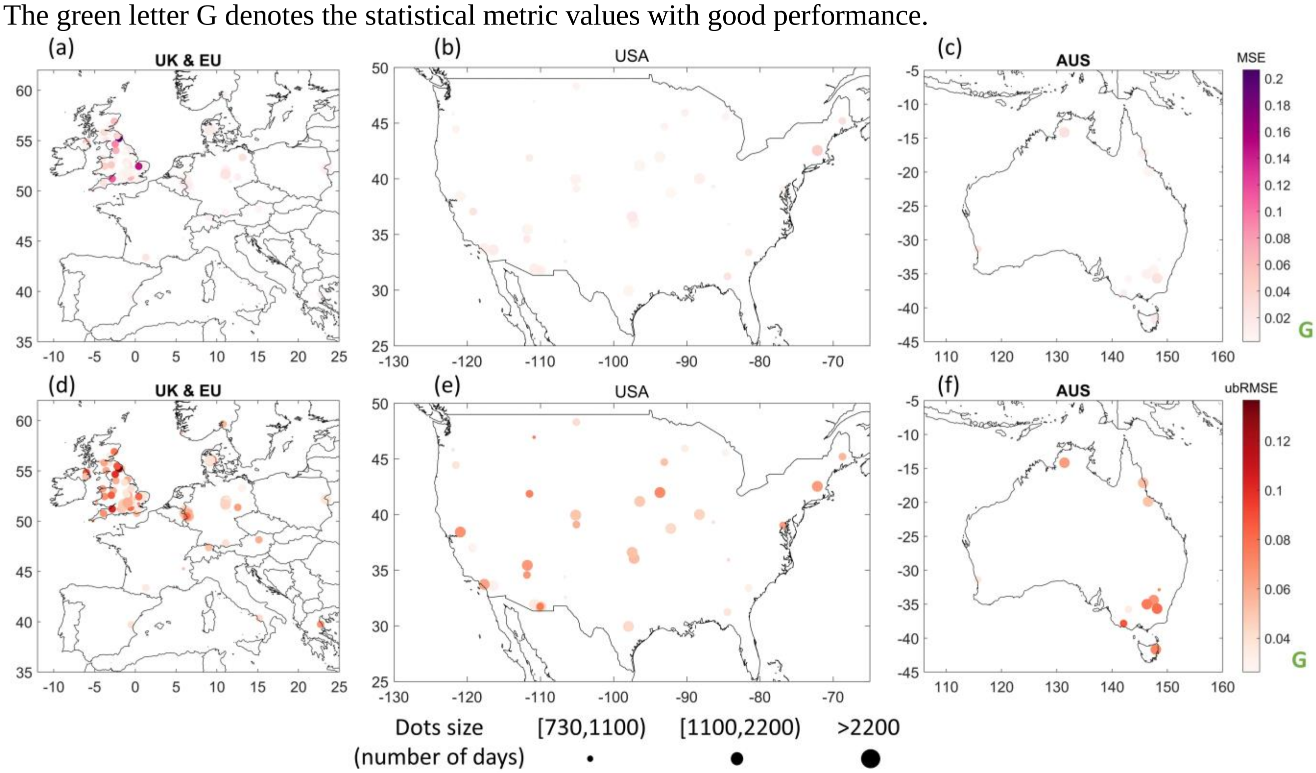

Figure S7. Spatial distribution of average statistical metrics *MSE* and *ubRMSE* performance of all 7 products. The green letter G denotes the statistical metric values with good performance.

Text S9. The performance of 6 statistical metrics under various soil properties

Figure S8 presents the spatial map of bulk density and soil organic carbon for CRNS sites used in this study. Most of the sites with low bulk density and high soil organic carbon are from the UK. Figure S9 demonstrates that all statistical metrics have worse performance in the sites with low bulk density and high soil organic carbon.

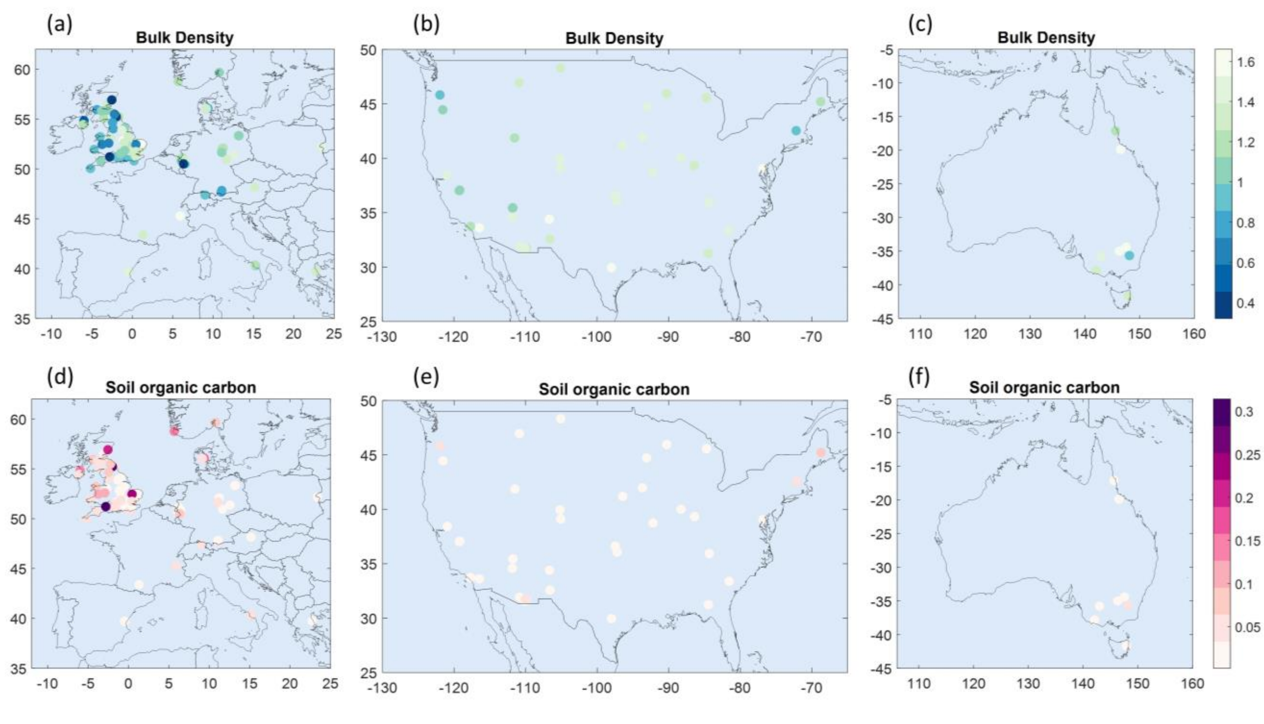

Figure S8. Spatial map of bulk density and soil organic carbon for CRNS sites used in this study.

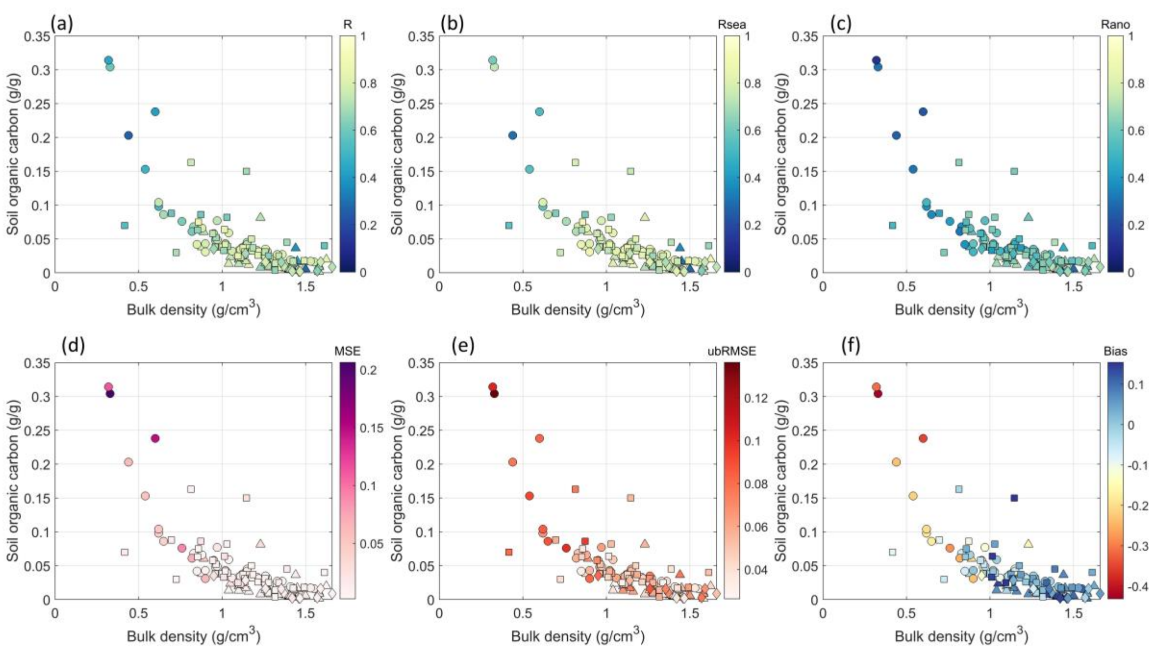

Figure S9. Statistical metrics performance under various bulk density and soil organic carbon conditions. The shape of the dots represents the CRNS sites from different networks (UK: circle; Europe: square; USA: triangle; Australia: diamond).

References:

Bogena, H. R., M. Schrön, J. Jakobi, P. Ney, S. Zacharias, M. Andreasen, R. Baatz, D. Boorman, M. B. Duygu and M. A. Eguibar-Galán (2022). "COSMOS-Europe: a European network of cosmic-ray neutron soil moisture sensors." *Earth System Science Data* **14**(3): 1125-1151.

Cooper, H. M., E. Bennett, J. Blake, E. Blyth, D. Boorman, E. Cooper, J. Evans, M. Fry, A. Jenkins and R. Morrison (2021). "COSMOS-UK: national soil moisture and hydrometeorology data for environmental science research." *Earth System Science Data* **13**(4): 1737-1757.

Evans, J., H. Ward, J. Blake, E. Hewitt, R. Morrison, M. Fry, L. Ball, L. Doughty, J. Libre and O. Hitt (2016). "Soil water content in southern England derived from a cosmic‐ray soil moisture observing system – COSMOS‐UK." *Hydrological Processes* **30**(26): 4987-4999.

Gelaro, R., W. McCarty, M. J. Suárez, R. Todling, A. Molod, L. Takacs, C. A. Randles, A. Darmenov, M. G. Bosilovich and R. Reichle (2017). "The modern-era retrospective analysis for research and applications, version 2 (MERRA-2)." *Journal of climate* **30**(14): 5419-5454.

GMAO, G. M. a. A. O. (2015). "MERRA-2 tavgM_2d_lnd_Nx: 2d,Monthly mean,Time-Averaged,Single-Level,Assimilation,Land Surface Diagnostics V5.12.4, Greenbelt, MD, USA." *Goddard Earth Sciences Data and Information Services Center (GES DISC)*(Accessed: 18 April 2022, 10.5067/8S35XF81C28F).

Gruber, A., G. De Lannoy, C. Albergel, A. Al-Yaari, L. Brocca, J.-C. Calvet, A. Colliander, M. Cosh, W. Crow and W. Dorigo (2020). "Validation practices for satellite soil moisture retrievals: What are (the) errors?" *Remote sensing of environment* **244**: 111806.

Hawdon, A., D. McJannet and J. Wallace (2014). "Calibration and correction procedures for cosmic‐ray neutron soil moisture probes located across Australia." *Water Resources Research* **50**(6): 5029-5043.

Kim, H., R. Parinussa, A. G. Konings, W. Wagner, M. H. Cosh, V. Lakshmi, M. Zohaib and M. Choi (2018). "Global-scale assessment and combination of SMAP with ASCAT (active) and AMSR2 (passive) soil moisture products." *Remote Sensing of Environment* **204**: 260-275.

Kobayashi, S., Y. Ota, Y. Harada, A. Ebita, M. Moriya, H. Onoda, K. Onogi, H. Kamahori, C. Kobayashi and H. Endo (2015). "The JRA-55 reanalysis: General specifications and basic characteristics." *Journal of the Meteorological Society of Japan. Ser. II* **93**(1): 5-48.

Köhli, M., M. Schrön, M. Zreda, U. Schmidt, P. Dietrich and S. Zacharias (2015). "Footprint characteristics revised for field‐scale soil moisture monitoring with cosmic‐ray neutrons." *Water Resources Research* **51**(7): 5772-5790.

Köhli, M., J. Weimar, M. Schrön, R. Baatz and U. Schmidt (2021). "Soil moisture and air humidity dependence of the above-ground cosmic-ray neutron intensity." *Frontiers in Water* **2**: 66.

Liu, Y. Y., R. M. Parinussa, W. A. Dorigo, R. A. M. De Jeu, W. Wagner, A. I. J. M. van Dijk, M. F. McCabe and J. P. Evans (2011). "Developing an improved soil moisture dataset by blending passive and active microwave satellite-based retrievals." *Hydrol. Earth Syst. Sci.* **15**(2): 425-436.

Liu, Z., C. Shi, Z. Zhou, L. Jiang, X. Liang, T. Zhang, J. Liao, J. Liu, M. Wang and S. Yao (2017). CMA global reanalysis (CRA-40): Status and plans. Proc. 5th International Conference on Reanalysis, Nat. Meteor. Int. Canter.

Martens, B., D. G. Miralles, H. Lievens, R. v. d. Schalie, R. A. De Jeu, D. Fernández-Prieto, H. E. Beck, W. A. Dorigo and N. E. Verhoest (2017). "GLEAM v3: Satellite-based land evaporation and root-zone soil moisture." *Geoscientific Model Development* **10**(5): 1903-1925.

Miralles, D., R. De Jeu, J. Gash, T. Holmes and A. Dolman (2011). "Magnitude and variability of land evaporation and its components at the global scale." *Hydrology and Earth System Sciences* **15**(3): 967-981.

Muñoz-Sabater, J., E. Dutra, A. Agustí-Panareda, C. Albergel, G. Arduini, G. Balsamo, S. Boussetta, M. Choulga, S. Harrigan and H. Hersbach (2021). "ERA5-Land: A state-of-the-art global reanalysis dataset for land applications." *Earth System Science Data* **13**(9): 4349-4383.

Power, D., M. A. Rico-Ramirez, S. Desilets, D. Desilets and R. Rosolem (2021). "Cosmic-Ray neutron Sensor PYthon tool (crspy 1.2.1): an open-source tool for the processing of cosmic-ray neutron and soil moisture data." *Geosci. Model Dev.* **14**(12): 7287-7307.

Reichle, R. H., C. S. Draper, Q. Liu, M. Girotto, S. P. P. Mahanama, R. D. Koster and G. J. M. De Lannoy (2017). "Assessment of MERRA-2 Land Surface Hydrology Estimates." *Journal of Climate* **30**(8): 2937-2960.

Rosolem, R., W. Shuttleworth, M. Zreda, T. E. Franz, X. Zeng and S. Kurc (2013). "The effect of atmospheric water vapor on neutron count in the cosmic-ray soil moisture observing system." *Journal of Hydrometeorology* **14**(5): 1659-1671.

Saha, S., S. Moorthi, H.-L. Pan, X. Wu, J. Wang, S. Nadiga, P. Tripp, R. Kistler, J. Woollen and D. Behringer (2010). "The NCEP climate forecast system reanalysis." *Bulletin of the American Meteorological Society* **91**(8): 1015-1058.

Saha, S., S. Moorthi, X. Wu, J. Wang, S. Nadiga, P. Tripp, D. Behringer, Y.-T. Hou, H.-y. Chuang and M. Iredell (2014). "The NCEP climate forecast system version 2." *Journal of climate* **27**(6): 2185-2208.

Xu, J., Z. Ma, S. Yan and J. Peng (2022). "Do ERA5 and ERA5-land precipitation estimates outperform satellite-based precipitation products? A comprehensive comparison between state-of-the-art model-based and satellite-based precipitation products over mainland China." *Journal of Hydrology* **605**: 127353.

Yu, X., L. Zhang, T. Zhou and J. Liu (2021). "The Asian Subtropical Westerly Jet Stream in CRA-40, ERA5, and CFSR Reanalysis Data: Comparative Assessment." *Journal of Meteorological Research* **35**(1): 46-63.

Yuan, X., E. F. Wood, L. Luo and M. Pan (2011). "A first look at Climate Forecast System version 2 (CFSv2) for hydrological seasonal prediction." *Geophysical research letters* **38**(13).

Yuan, X., E. F. Wood, J. K. Roundy and M. Pan (2013). "CFSv2-based seasonal hydroclimatic forecasts over the conterminous United States." *Journal of Climate* **26**(13): 4828-4847.

Zhao, D., L. Zhang, T. Zhou and J. Liu (2021). "Contributions of Local and Remote Atmospheric Moisture Fluxes to East China Precipitation Estimated from CRA-40 Reanalysis." *Journal of Meteorological Research* **35**(1): 32-45.

Table S2. List of the 135 CRNS sites used in this study.

CRNS site name	Station ID	Country	Latitude	Longitude	Elevation (m)	Reclassified land cover	Start date
Manitou Forest Tower	USA_SITE_004	USA	39.10	-105.10	2411	Forest	10/2009
Marshall Colorado	USA_SITE_006	USA	39.95	-105.20	1756	Cropland	10/2009
Kendall	USA_SITE_010	USA	31.74	-109.94	1548	Shrubland	06/2010
Santa Rita Creosote	USA_SITE_011	USA	31.91	-110.84	989	Shrubland	06/2010
SMAP-OK	USA_SITE_014	USA	36.06	-97.22	326	Grassland	07/2010
ARM-1	USA_SITE_015	USA	36.61	-97.49	322	Cropland	07/2010
Iowa Validation Site	USA_SITE_016	USA	41.98	-93.68	316	Cropland	09/2010
San Pedro 2	USA_SITE_020	USA	31.56	-110.14	1233	Shrubland	01/2011
Desert Chaparral UCI	USA_SITE_023	USA	33.61	-116.45	1292	Shrubland	03/2011
Coastal Sage UCI	USA_SITE_024	USA	33.73	-117.70	320	Shrubland	03/2011
Chestnut Ridge NOAA	USA_SITE_025	USA	35.93	-84.33	370	Forest	03/2011
Bondville	USA_SITE_026	USA	40.01	-88.29	219	Cropland	03/2011
Morgan Monroe	USA_SITE_027	USA	39.32	-86.41	275	Forest	03/2011
Mozark	USA_SITE_028	USA	38.74	-92.20	219	Forest	04/2011
Neb Field 3	USA_SITE_029	USA	41.18	-96.44	363	Cropland	04/2011
Harvard Forest	USA_SITE_030	USA	42.54	-72.17	350	Forest	05/2011
Howland	USA_SITE_031	USA	45.20	-68.74	124	Forest	05/2011
Tonzi Ranch	USA_SITE_032	USA	38.43	-120.97	177	Shrubland	05/2011
Soaproot	USA_SITE_033	USA	37.03	-119.26	1160	Forest	06/2011
P301	USA_SITE_034	USA	37.07	-119.19	2014	Forest	06/2011
Wind River	USA_SITE_035	USA	45.82	-121.95	371	Forest	06/2011
Hauser Farm South	USA_SITE_037	USA	34.58	-111.86	942	Cropland	06/2011
Metolius	USA_SITE_038	USA	44.45	-121.56	1253	Forest	06/2011
Rosemount	USA_SITE_041	USA	44.71	-93.09	260	Cropland	07/2011
Park Falls	USA_SITE_042	USA	45.95	-90.27	470	Forest	07/2011
UMBS	USA_SITE_043	USA	45.56	-84.71	220	Forest	07/2011

Daniel Forest	USA_SITE_046	USA	41.87	-111.51	2600	Forest	08/2011
Tenderfoot Creek	USA_SITE_047	USA	46.95	-110.89	2255	Forest	08/2011
Fort Peck	USA_SITE_048	USA	48.31	-105.10	634	Grassland	08/2011
JERC	USA_SITE_052	USA	31.24	-84.46	40	Forest	09/2011
Savannah River	USA_SITE_053	USA	33.38	-81.57	94	Forest	09/2011
Freeman Ranch	USA_SITE_057	USA	29.95	-98.00	265	Forest	10/2011
Sevilleta New Grass	USA_SITE_058	USA	34.40	-106.67	1566	Shrubland	02/2012
Lucky Hills	USA_SITE_060	USA	31.74	-110.05	1367	Shrubland	03/2012
Flag Wildfire	USA_SITE_061	USA	35.45	-111.77	2313	Shrubland	04/2012
Flag Ponderosa Pine	USA_SITE_062	USA	35.44	-111.80	2381	Forest	04/2012
Beltsville	USA_SITE_065	USA	39.03	-76.85	42	Grassland	04/2012
Jornada Mixed Shrubland	USA_SITE_072	USA	32.58	-106.60	0	Shrubland	01/2013
AliceHolt	ALIC1	UK	51.15	-0.86	80	Forest	06/2015
Balruddery	BALRD	UK	56.48	-3.11	130	Cropland	05/2014
BickleyHall	BICKL	UK	53.03	-2.70	78	Grassland	01/2015
BunnyPark	BUNNY	UK	52.86	-1.13	39	Cropland	01/2015
Cardington	CARDT	UK	52.11	-0.42	29	Cropland	06/2015
ChimneyMeadows	CHIMN	UK	51.71	-1.48	65	Grassland	02/2013
ChobhamCommon	CHOBH	UK	51.37	-0.60	47	Forest	02/2015
Cochno	COCHN	UK	55.94	-4.40	168	Grassland	08/2017
CocklePark	COCLP	UK	55.22	-1.69	87	Cropland	11/2014
Crichton	CRICH	UK	55.04	-3.58	42	Grassland	02/2014
CwmGarw	CGARW	UK	51.95	-4.75	299	Grassland	06/2016
EasterBush	EASTB	UK	55.87	-3.21	208	Grassland	08/2014
Elmsett	ELMST	UK	52.09	0.99	76	Cropland	11/2016
Euston	EUSTN	UK	52.34	0.80	18	Cropland	03/2016
Fincham	FINCH	UK	52.62	0.51	15	Cropland	07/2017
GisburnForest	GISBN	UK	54.02	-2.38	246	Forest	08/2014
Glensaugh	GLENS	UK	56.91	-2.56	399	Shrubland	05/2014

Glenwherry	GLENW	UK	54.84	-6.00	274	Grassland	06/2016
Hadlow	HADLW	UK	51.23	0.32	33	Cropland	10/2016
HartwoodHome	HARTW	UK	55.81	-3.83	225	Grassland	05/2014
HarwoodForest	HARWD	UK	55.22	-2.02	300	Forest	05/2015
HenfaesFarm	HENFS	UK	53.23	-4.01	287	Shrubland	12/2015
Heytesbury	HYBRY	UK	51.20	-2.08	166	Grassland	08/2017
Hillsborough	HILLB	UK	54.45	-6.07	146	Grassland	06/2016
HollinHill	HOLLN	UK	54.11	-0.96	82	Cropland	03/2014
Loddington	LODTN	UK	52.61	-0.83	186	Cropland	04/2016
LullingtonHeath	LULLN	UK	50.79	0.19	119	Grassland	12/2014
MoorHouse	MOORH	UK	54.66	-2.47	565	Grassland	04/2014
Morley	MORLY	UK	52.55	1.03	55	Cropland	05/2014
NorthWyke	NWYKE	UK	50.77	-3.91	181	Grassland	10/2014
Plynlimon	PLYNL	UK	52.45	-3.76	542	Grassland	05/2014
PortonDown	PORTN	UK	51.12	-1.68	146	Grassland	12/2014
Redhill	REDHL	UK	51.26	0.43	91	Grassland	02/2016
Redmere	RDMER	UK	52.45	0.42	3	Shrubland	10/2015
Riseholme	RISEH	UK	53.26	-0.53	53	Grassland	04/2016
Rothamsted	ROTHD	UK	51.81	-0.38	131	Cropland	07/2014
Sheepdrove	SHEEP	UK	51.53	-1.48	170	Cropland	10/2013
Sourhope	SOURH	UK	55.48	-2.23	487	Grassland	11/2014
SpenFarm	SPENF	UK	53.87	-1.32	57	Cropland	11/2016
Stiperstones	STIPS	UK	52.58	-2.94	432	Grassland	06/2014
Stoughton	STGHT	UK	52.60	-1.05	130	Cropland	08/2015
TadhamMoor	TADHM	UK	51.21	-2.83	7	Grassland	10/2014
TheLizard	LIZRD	UK	50.03	-5.20	85	Shrubland	10/2014
Waddesdon	WADDN	UK	51.84	-0.95	98	Grassland	04/2013
Writtle	WRTTL	UK	51.73	0.42	44	Cropland	04/2017
Aas	AAC001	Norway	59.66	10.76	72	Grassland	09/2016

Acheleschwaig	ACC001	Germany	47.67	10.99	867	Grassland	06/2017
Agia	AGCK003	Greece	39.76	22.72	1032	Shrubland	03/2017
Alento1	ALC001	Italy	40.31	15.23	671	Forest	02/2016
Alento2	ALC002	Italy	40.37	15.18	453	Cropland	02/2016
Calderona1	CAC001	Spain	39.71	-0.46	785	Shrubland	10/2016
Crolles	CRC001	France	45.28	5.90	230	Grassland	07/2016
Cunnersdorf	CUC001	Germany	51.37	12.56	140	Cropland	06/2016
Derlo	DEC001	Poland	52.17	23.37	129	Grassland	04/2013
Fendt	FEC001	Germany	47.83	11.06	595	Grassland	06/2015
Fuerstensee	FSC001	Germany	53.32	13.12	66	Grassland	01/2014
Grosses Bruch	GBC001	Germany	52.03	11.11	80	Cropland	07/2014
Gludsted	GLC001	Denmark	56.07	9.33	86	Forest	02/2013
Harrild	HAC001	Denmark	56.02	9.16	66	Shrubland	03/2014
Hordorf	HDC001	Germany	52.00	11.18	82	Cropland	06/2020
Serrahn	HHC001	Germany	53.34	13.17	96	Forest	08/2016
Hohes Holz	HOC001	Germany	52.09	11.23	217	Forest	08/2014
Jena	JEC001	Germany	50.95	11.63	140	Grassland	03/2015
Merzenhausen	MEBCK001	Germany	50.93	6.30	91	Cropland	02/2011
Olocau	OLC001	Spain	39.71	-0.52	415	Shrubland	01/2017
Petzenkirchen	PEC001	Austria	48.16	15.15	278	Cropland	12/2013
Rietholzbach	RIC001	Switzerland	47.38	8.99	755	Grassland	12/2010
Rollesbroich1	ROC001	Germany	50.62	6.30	515	Grassland	05/2011
Rollesbroich2	ROC002	Germany	50.62	6.31	506	Grassland	07/2012
Schoeneseiffen	RUBCDKR001	Germany	50.52	6.38	611	Grassland	08/2015
Gevenich	RUBCK002	Germany	50.99	6.32	107	Cropland	07/2011
Ruraue	RUBCK003	Germany	50.86	6.43	100	Grassland	11/2011
Wildenrath	RUBCK004	Germany	51.13	6.17	72	Forest	04/2012
Heinsberg	RUC004	Germany	51.04	6.10	58	Cropland	09/2011
Kall	RUC005	Germany	50.50	6.53	505	Grassland	09/2011

Aachen	RUC006	Germany	50.80	6.03	232	Cropland	01/2012
Kleinhau1	RUC007	Germany	50.72	6.37	374	Grassland	08/2015
Saerheim	SAC001	Norway	58.76	5.65	91	Grassland	09/2017
Schaefertal1	SCC001	Germany	51.66	11.04	425	Cropland	10/2010
Schaefertal4	SCC004	Germany	51.66	11.05	399	Cropland	09/2010
Selhausen	SEC001	Germany	50.87	6.45	101	Cropland	03/2015
Toulouse	TOC001	France	43.39	1.29	188	Grassland	02/2011
Voulund	VOC001	Denmark	56.04	9.16	67	Cropland	02/2013
Wildacker	WAC001	Germany	53.33	13.20	96	Forest	07/2013
Wuestebach1	WUC001	Germany	50.50	6.33	605	Forest	02/2011
Wuestebach2	WUC002	Germany	50.51	6.33	607	Forest	06/2014
Baldry	AUS_SITE_001	Australia	-32.87	148.53	438	Shrubland	03/2011
Daly	AUS_SITE_002	Australia	-14.16	131.39	75	Shrubland	06/2011
Gnangara	AUS_SITE_003	Australia	-31.38	115.71	50	Forest	05/2011
Robson	AUS_SITE_006	Australia	-17.12	145.63	715	Forest	10/2010
Temora	AUS_SITE_007	Australia	-34.40	147.53	294	Cropland	05/2013
Tullochgorum	AUS_SITE_008	Australia	-41.67	147.91	285	Cropland	12/2010
Tumbarumba	AUS_SITE_009	Australia	-35.66	148.15	1200	Forest	04/2011
Weany Creek	AUS_SITE_010	Australia	-19.88	146.54	287	Grassland	12/2010
Yanco	AUS_SITE_011	Australia	-35.01	146.30	124	Cropland	04/2011
Hamilton	AUS_SITE_015	Australia	-37.83	142.09	119	Cropland	07/2015
Bishes	AUS_SITE_018	Australia	-35.77	142.97	94	Cropland	04/2016